Facilitated Transport of Molecular Oxygen in the Membranes of Polymer-Coordinated Cobalt Schiff Base Complexes

Eishun Tsuchida,* Hiroyuki Nishide, Manshi Ohyanagi, and Hiroyoshi Kawakami

Department of Polymer Chemistry, Waseda University, Tokyo 160, Japan.
Received October 1, 1986

ABSTRACT: (*N,N'*-Disalicylideneethylenediamine)cobalt(II) (CoS) forms a five-coordinate complex with poly[(octyl methacrylate)-*co*-(4-vinylpyridine)] (POMPy) or poly[(octyl methacrylate)-*co*-(1-vinylimidazole)] (POMIm), which binds molecular oxygen rapidly and reversibly even in the solid state through the vacant sixth coordination site. In the membranes of these polymer-coordinated CoS complexes molecular oxygen transport is facilitated, because the CoS complex effectively acts as a fixed carrier for the oxygen transport in the membranes. Oxygen-binding parameters determined spectroscopically were adequate to analyze the dual-mode transport model, by which the oxygen permeation behaviors are quantitatively discussed. Effects of the oxygen-binding capability and of the concentration of the CoS fixed carrier on the facilitated oxygen transport are also discussed by using the model.

Introduction

Much progress recently has been made in the study of oxygen-enriching membranes.[1] Most of the attention for such membranes has been focused on the syntheses of polymers in which the solubility coefficient of oxygen is greater than that for nitrogen.[2] However, no permselective membrane has been successfully prepared by using this approach.

On the other hand, the design of a polymer containing a carrier which interacts specifically and reversibly with oxygen presents an interesting approach to the preparation of an oxygen permselective membrane. The present authors recently have reported preparation of the polymer membranes containing a cobalt porphyrin complex[3] and a cobalt Schiff base complex[4] as the fixed carrier of oxygen which sorb and transport oxygen selectively by means of the Langmuir mode and in which oxygen transport is enhanced.

The present paper describes the selective and dual-mode transport of molecular oxygen in the membranes of polymer-coordinated cobalt Schiff base (Chart I). The polymer membranes have been prepared by homogeneously complexing (*N,N'*-disalicylideneethylenediamine)cobalt(II) (CoS) to poly[(octyl methacrylate)-*co*-(4-vinylpyridine)] (POMPy) and poly[(octyl methacrylate)-*co*-(1-vinylimidazole)] (POMIm). The coordination structure and rapid and reversible oxygen-binding capability of the polymer-coordinated CoS complex (the fixed carrier) in the membrane state have been characterized by means of spectroscopic methods. Oxygen permeation behavior was measured in connection with the upstream oxygen pressure and is discussed in terms of the combination of dual-mode transport theory[5] and the spectroscopic data. The discussion also includes effects of the oxygen-binding capability and the concentration of the CoS complex as the fixed carrier on the facilitated oxygen transport in the membrane.

Experimental Section

Materials. (*N,N'*-Disalicylideneethylenediamine)cobalt(II) (CoS) was synthesized by literature methods.[6] Poly[(octyl methacrylate)-*co*-4-(vinylpyridine)] (POMPy) and poly[(octyl methacrylate)-*co*-1-(vinylimidazole)] (POMIm) were prepared by the radical copolymerization of octyl methacrylate and 4-vinylpyridine and 1-vinylimidazole initiated by azobisisobutyronitrile. Vinylpyridine and vinylimidazole residue content and molecular weight of the copolymers were determined to be 15 mol %, 1.5×10^5 for POMPy and 12 mol %, 1.0×10^5 for POMIm, by elemental analysis and gel-permeation chromatography (with tetrahydrofuran as the solvent and polystyrene as the standard), respectively. The toluene solution of the copolymer and CoS was carefully cast on a Teflon plate under an atmosphere free of oxygen, and then dried in vacuo, to yield a transparent and flexible membrane with thickness of ca. 60 μm.

Chart I

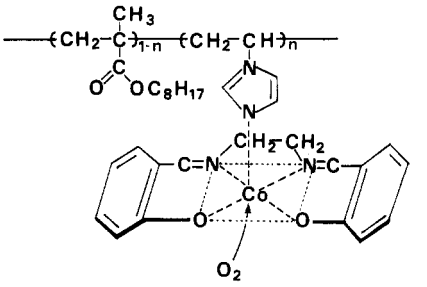

Spectroscopic Measurements. Reversible oxygen-binding to the CoS complex in the membrane was observed with spectral changes in the visible absorption, using a high-sensitivity Shimazu UV-2000 spectrophotometer.

Coordination structure of the polymer-coordinated CoS complex was studied by ESR (electron spin resonance) spectroscopy (JEOL FE-3X spectrometer operating at X-band at 77 K and room temperature), using a sample tube with a vessel for deaeration. Tetracyanoquinodimethane was used as an external standard (g = 2.0026).

Permeation Measurement. Oxygen permeation coefficient for various upstream gas pressures was measured with a low-vacuum permeation apparatus (Rika Seiki Inc. Type K-315 N-03) at a constant temperature. The pressure on the upstream side was maintained essentially constant. The pressures on the upstream and the downstream side were detected by using Baratron's absolute pressure gauge (MKS Instruments Inc.). The membrane was set in the apparatus and kept in vacuo over a half day before the measurement to exclude gas leakage. Nitrogen permeation coefficients were measured by the same procedure as for oxygen.

Results and Discussion

Structure of the Polymer-Coordinated CoS Complex. The typical ESR spectrum of the POMPy–CoS complex is shown in Figure 1a in frozen toluene glass (T = 77 K) (g_x = 2.45, g_y = 2.216, g_z = 2.015). The spectrum shows no axial symmetry around the cobalt(II) ion; in the lower field region a rhombic distortion splitting is observed, which is characteristic for Co(II) complexes with equatorial N_2O_2 ligands such as CoS. Three superhyperfine splitting lines are observed in the hyperfine lines at the higher magnetic field. This is based on the coordination of a single nitrogen nucleus as an axial ligand, indicating the formation of a five-coordinate CoS complex.

0024-9297/87/2220-1907$01.50/0

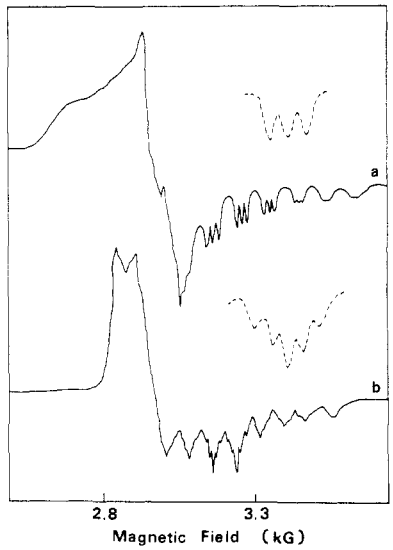

Figure 1. ESR spectra of the POMPy–$Co^{II}S$ complex (a) and the Py–$Co^{II}S$ complex (b) in toluene glass at 77 K. The dotted lines show enlarged spectra.

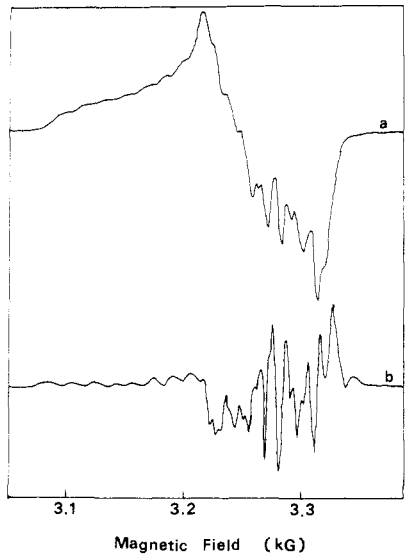

Figure 2. ESR spectrum of the POMPy–$Co^{II}S$–O_2 adduct in toluene glass at 77 K: (a) normal absorption derivative; (b) its second derivative.

The $Co^{II}S$ complex with low molecular weight pyridine exhibits a different ESR spectrum as shown in Figure 1b (g_x = 2.33, g_y = 2.263, g_z = 2.029). Several hyperfine structure lines are split into five superhyperfine lines with the intensity of 1:2:3:2:1. This indicates a six-coordinate structure which contains two equivalent nitrogen nuclei of pyridine coordinated to the fifth and sixth coordination sites of $Co^{II}S$, which is in accordance with the previously reported structure[7] of the CoS complex with nitrogenous ligands. Polymer nitrogenous ligands such as POMPy form preferentially the five-coordinate CoS complex probably because steric hindrance of the five-coordinated polymer chain suppresses coordination in the sixth site by the same bulky polymer chain. Regardless, POMPy forms the five coordinate CoS complex, which leaves the sixth coordination site vacant and able to bind molecular oxygen rapidly.

POMIm gives a similar spectrum; however, the superhyperfine splitting was not clearly observed. This suggests that a six-coordinate CoS complex with no oxygen-binding ability coexists with the active five-coordinate one for the POMIm–CoS complex.

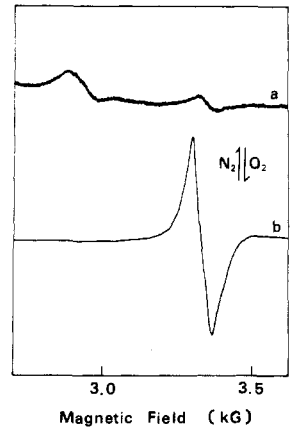

Figure 3. Reversible ESR spectral change of the POMPy–$Co^{II}S$ complex in toluene at 25 °C.

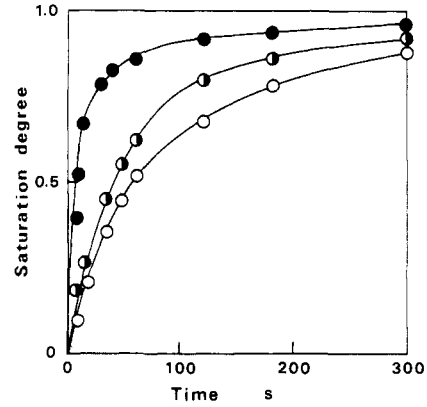

Figure 4. Time course of the oxygen adsorption in the POMIm–CoS membrane at 35 °C; $p_2(O_2)$ = 25 (○), 70 (◑), 760 mmHg (●); [CoS] = 0.6 wt %.

Figure 2 shows the spectrum of POMPy–$Co^{II}S$ in frozen toluene glass in the presence of oxygen. The spectrum shows a small rhombic distortion and eight-line hyperfine splitting patterns are observed in the second derivative of the spectrum (g_x = 2.001, g_y = 2.007, g_z = 2.085). This indicates formation of an oxygen adduct (O_2/Co = 1/1 adduct).

Oxygen Binding to the Complex in the Membrane. When the membranes of the POMPy–CoS and POMIm–CoS complex are exposed to oxygen, oxygen-binding to the CoS complexes in the membrane can be monitored by visible absorption and ESR spectroscopic techniques. Figure 3 shows the ESR spectral change. A new strong signal assigned to the oxygen adduct develops in the vicinity of g = 2 as the membrane is exposed to oxygen at room temperature.

Color of the membranes also changed reversibly from brown under nitrogen to deep violet on exposure to oxygen. The spectral change of the membrane agreed with that of the polymer CoS complex in solution previously reported:[8] UV and visible absorption maxima λ_{max} = 555 nm (oxy), λ_{max} = 345, 405 nm (deoxy; five coordination), and isosbestic points at 335, 410 nm for the POMIm–CoS membrane and λ_{max} = 545 nm (oxy), λ_{max} = 345, 402 nm (deoxy), and isosbestic points at 335, 410 nm for the POMPy–CoS membrane.

The reversible oxy–deoxy spectral change occurs rapidly; e.g., for the 60-μm-thick membranes containing 0.6 wt % CoS, 90% of the oxygen-binding was established within a few minutes after the exposure to oxygen at 35 °C (Figure 4). It is important for a fixed carrier of oxygen that oxygen be sorbed and desorbed rapidly in response

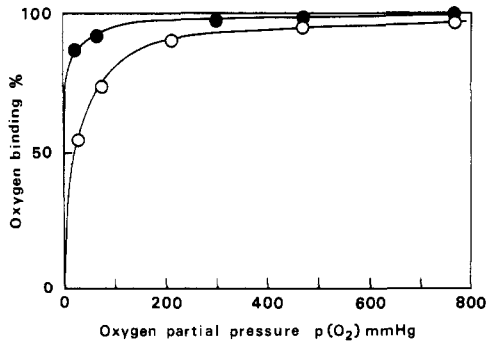

Figure 5. Oxygen-binding equilibrium curves for the POMIm–CoS membrane (●) and the POMPy–CoS membrane (○), at 25 °C; [CoS] = 0.6 wt %.

Table I
Oxygen-Binding Equilibrium Constants[a] and Thermodynamic Parameters[b] for the POMPy–CoS and POMIm–CoS Membrane

polymer	K, $cmHg^{-1}$	ΔH, kcal mol^{-1}	ΔS, eu
POMPy	0.68	−15	−44
POMIm	2.5	−22	−66

[a] Data at 25 °C. [b] Data from Figure 5 (ln K in atm^{-1}).

Table II
Oxygen-Binding Rate Constants[a] and Thermodynamic Parameters for the POMPy–CoS and POMIm–CoS Membrane

polymer	k_{on}, $mmHg^{-1}$ s^{-1}	k_{off}, s^{-1}	$E_{a,on}$, kcal mol^{-1}	$E_{a,off}$, kcal mol^{-1}
POMPy	6.8×10^{-5}	1.1×10^{-3}	7.1	24
POMIm	5.8×10^{-5}	2.3×10^{-4}	23	47

[a] Apparent rate constants (thickness of the membranes; 60 μm) at 25 °C.

to a change in partial oxygen pressure even after the fixation in a feasible membrane.

POMPy (or POMIm)–CoS +

$$O_2 \underset{k_{off}}{\overset{k_{on}}{\rightleftharpoons}} \text{POMPy (or POMIm)–CoS–O}_2 \quad (1)$$

The oxygen-binding equilibrium constants ($K = k_{on}/k_{off}$) were determined by conducting the oxygen-binding and -dissociation equilibrium measurement as in the previous papers.[3,4] The Langmuir-type oxygen-binding equilibrium curves and the K values are given in Figure 5 andTable I, respectively. Thermodynamic parameters for the oxygen binding were determined from the temperature dependence of K (van't Hoff plots; Figure 6) and also are given in Table I. The K value of POMIm–CoS, of which the fifth and axial ligand is an imidazole derivative with stronger basicity in comparison with that of a pyridine derivative, is larger than that of the POMPy–CoS membrane at the measuring temperature.

Apparent k_{on} and k_{off} have been estimated by analyzing time courses of the oxygen adsorption (Figure 4) according to pseudo-first-order kinetic treatment based upon the kinetic equation of the Langmuir isotherm and listed in Table II. The k_{off} value of POMPy–CoS is larger than that for POMIm–CoS at 25 °C, although the former approaches the latter at higher temperature. One of the advantages for the membrane containing the CoS complex as the fixed carrier is that the oxygen-binding capability, i.e., the oxygen-binding rate constant and equilibrium constant, of the complex is able to be changed by the fifth coordinated nitrogenous ligand of CoS. Effect of the oxygen-binding capability of the fixed carrier on the oxygen transport is discussed below.

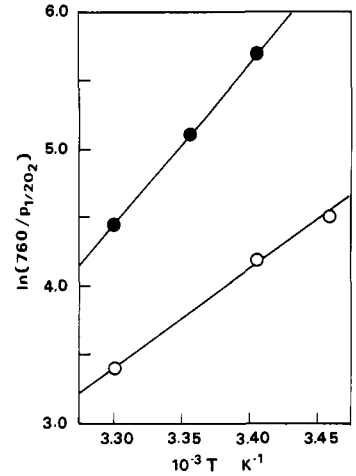

Figure 6. van't Hoff plots of the oxygen-binding equilibrium constants for the POMIm–CoS membrane (●) and the POMPy-CoS membrane (○); [CoS] = 0.6 wt %.

Oxygen Permeability in the Fixed Carrier Membrane. Oxygen sorption and desorption to and from the CoS complex in the membranes were rapid and according to the Langmuir isotherm. It is expected that oxygen is not immobilized to the CoS complex during the passage through the membrane and that oxygen transport is facilitated by the additional Langmuir mode transport, as has been reported by us for the membrane containing a cobalt porphyrin complex as a fixed carrier.[3] That is, the oxygen permeation coefficient is represented as the sum of the Henry mode and the Langmuir mode transport (eq 2[5]). Here, P is the permeability coefficient, k_D is the

$$P = k_D D_D(1 + FR/(1 + Kp_2)) \quad (2)$$

$$F = D_C/D_D; \qquad R = C'_C K/k_D$$

solubility coefficient for Henry's law, D_D and D_C are the diffusion coefficients for the Henry and the Langmuir-type diffusion, C'_C is the saturated amount of oxygen reversibly bound to the binding site or fixed carrier and is expected to be constant in this case, K is the oxygen-binding and -dissociation equilibrium constant, and p_2 is the upstream gas pressure. Eq 2 is a function of p_2 and P increases with a decrease in p_2 if the CoS complex as a fixed carrier acts effectively as the Langmuir-type sorption site.

Figure 7 shows the effect of upstream gas pressure (p_2) on the permeability coefficients (P_{O_2} and P_{N_2}) in the POMIm membrane complexed with 0.6 wt % CoS. Although the dependence of P on p_2 often has been reported for glassy polymers,[5b] the glass transition temperature is −4 °C for the POMIm–CoS membrane, and the membrane was in a rubbery state at the temperatures for the permeability measurement. In fact P_{N_2} is independent of $p_2(N_2)$ because the fixed carrier does not interact with nitrogen. Furthermore, the P_{O_2} values are independent of $p_2(O_2)$ for the POMIm membrane not containing CoS and for the POMIm–Co^{III}S membrane (the corresponding Co(III) complex of CoS does not interact with oxygen).

P_{O_2} obviously increases with a decrease in $p_2(O_2)$ in Figure 7, which suggests that oxygen transport occurs by the dual mode. As has been shown in Table I, the oxygen-binding affinity, K, of the POMIm–CoS complex decreases with temperature. Thus it is assumed that contribution of the Langmuir population decreases with temperature. However, the $p_2(O_2)$ dependency of P_{O_2} is rather enhanced at higher temperature as is seen in Figure 7. At 25 °C P_{O_2} is not affected by $p_2(O_2)$, which means that the

Table III
Dual-Mode Transport Parameters for the POMPy-CoS and POMIm-CoS Membrane

polymer	T, °C	D_D, cm²/s	D_C, cm²/s	$F(D_C/D_D)$	k_D, cm³(STP)/cm³ cmHg	C'_C, cm³(STP)/cm³	K, 1/cmHg
POMPy	25	1.4×10^{-6}	1.7×10^{-8}	0.01	9.8×10^{-4}	0.2	6.8×10^{-1}
	35	2.6×10^{-6}	3.6×10^{-8}	0.01	7.4×10^{-4}	0.2	2.6×10^{-1}
	45	4.8×10^{-6}	8.5×10^{-8}	0.02	5.8×10^{-4}	0.2	1.1×10^{-1}
POMIm	25	1.2×10^{-6}	0	0	1.3×10^{-3}	0.1	2.5
	35	4.8×10^{-6}	8.2×10^{-8}	0.02	4.6×10^{-4}	0.1	5.4×10^{-1}
	45	8.9×10^{-6}	2.5×10^{-7}	0.03	3.5×10^{-4}	0.1	2.0×10^{-1}

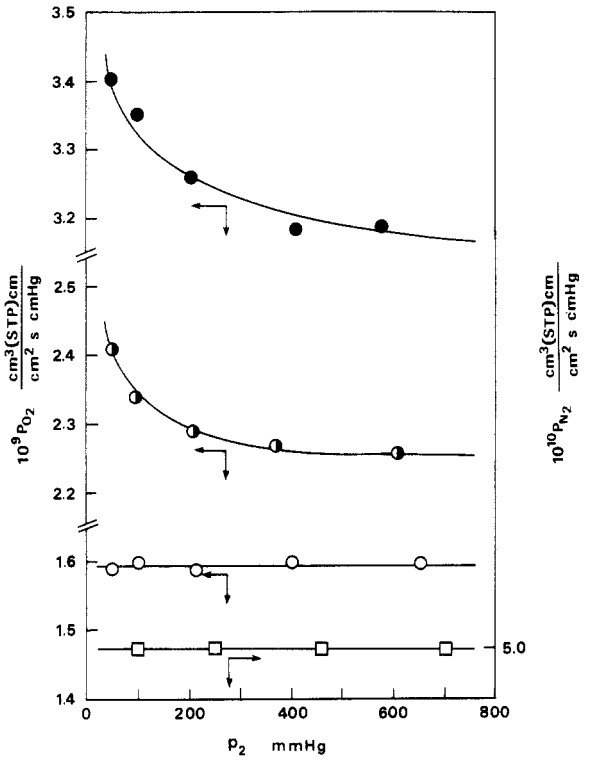

Figure 7. Effect of upstream gas pressure on permeation coefficient for the POMIm-CoS membrane: oxygen at 25 (○), 35 (◑), 45 °C (●); nitrogen at 25 °C (□); [CoS] = 0.6 wt %.

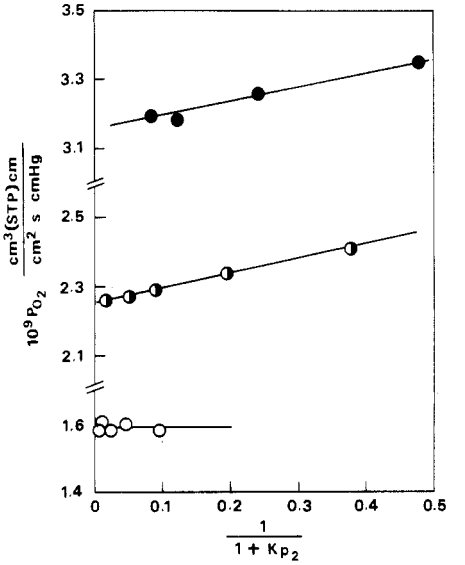

Figure 8. Oxygen permeability in the POMIm-CoS membrane plotted according to eq 2: (○) 25, (◑) 35, (●) 45 °C.

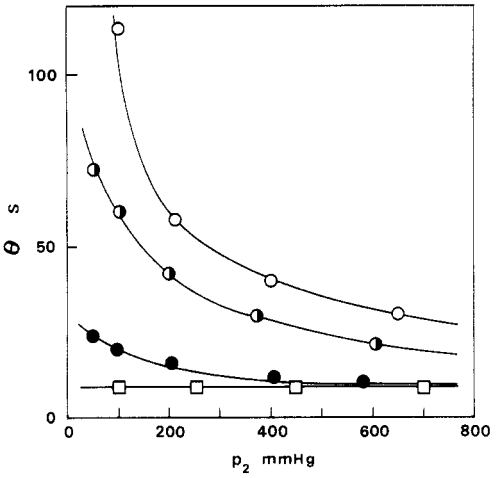

Figure 9. Effect of upstream gas pressure on time lag for the POMIm-CoS membrane: oxygen at 25 (○), 35 (◑), 45 °C (●); nitrogen at (□) 25 °C.

Langmuir-sorbed oxygen is totally immobilized on the fixed carrier. It is considered that the oxygen desorption rate from the CoS complex is much reduced with a decrease in temperature (see Table II) and that this kinetic property of CoS in the oxygen-binding predominantly influences the oxygen-transport phenomenon in comparison with the property of CoS in the oxygen-binding equilibrium (affinity). That is, an increase of F ($=D_C/D_D$) in eq 2 with temperature contributes to the facilitated transport of oxygen via the fixed carrier. Actually the F values of ~0 and 0.03 at 25 and 45 °C, respectively, as mentioned later (see Table III).

The effect of $p_2(O_2)$ on P_{O_2} was analyzed by using eq 2, that is, P_{O_2} was plotted against $1/(1 + Kp_2)$ (Figure 8). The plots show a linear relationship. The oxygen permeability in the POMIm membrane complexed with the CoS complex as a fixed carrier can be explained in terms of the sum of the Henry mode attributed to the polymer matrix and the Langmuir mode attributed to the fixed carrier, that is, the dual-mode theory.

Time course of gaseous molecule permeation through membranes often shows an induction period (time lag) followed by a permeation with a constant slope (steady state). For a fixed carrier membrane the time lag in the permeation-time course should be enhanced because the fixed carrier interacts with the penetrant and retards its diffusivity into the membrane. The oxygen permeation time lag for the membrane containing the CoS complex is also governed by both the Henry and the Langmuir mode.

The time lag (θ) for oxygen permeation also depends on $p_2(O_2)$, as shown in Figure 9, in the same manner as the permeation coefficient. This behavior indicates that oxygen clearly interacts with the CoS complex in the POMIm membrane. This is further supported by the results that θ is independent of the upstream gas pressures for nitrogen permeation in the POMIm-CoS membrane, oxygen permeation in the POMIm membrane not containing CoS, and oxygen permeation in the POMIm-inert $Co^{III}S$ membrane. In Figure 9 one also notices that θ_{O_2} and the $p_2(O_2)$ dependency of θ_{O_2} decrease with temperature. θ_{O_2} and the

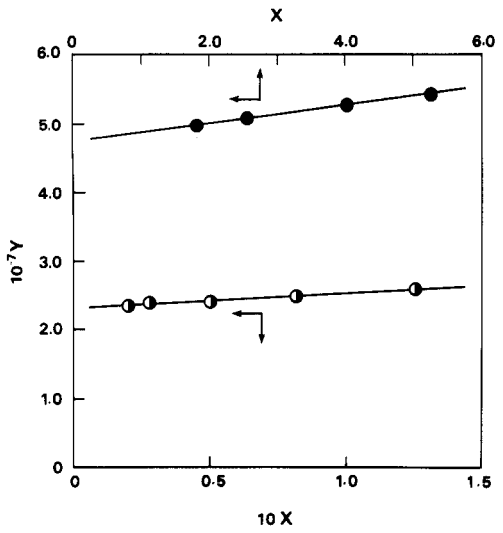

Figure 10. Oxygen permeability parameters in the POMIm–CoS membrane plotted according to eq 3: 35 (◑), 45 °C (●).

$p_2(O_2)$ dependency of θ_{O_2} are based on oxygen binding to the fixed carrier and enhanced at lower temperature because the oxygen binding equilibrium constant (K) of the fixed carrier increases and the desorption rate constant (k_{off}) decreases with a decrease in temperature (see Table I).

The effect of $p_2(O_2)$ on the time lag was analyzed by using the theoretical equation (eq 3):[3b] the FR value was calculated from the slope and the intercept of the linear relationship in Figure 6 and was substituted in eq 3; the

$$\frac{6\theta[1 + FR/(1 + y)]^3}{[f_0(y) + FRf_1(y) + (FR)^2f_2(y)]l^2}(Y) = \frac{R}{D_D} + \frac{1 + FRf_3(y) + (FR)^2f_4(y)}{f_0(y) + FRf_1(y) + (FR)^2f_2(y)}(X)\frac{1}{D_D}$$

$$F = D_C/D_D, \quad R = C'_CK/k_D, \quad y = Kp_2, \quad l = \text{thickness of membrane} \quad (3)$$

left term (Y) was plotted against the right term (X) (Figure 10), to give also a linear relationship, which also supports the dual-mode transport of oxygen in the membrane and a pathway of oxygen permeation via the fixed carrier. The functions of y, $f_0(y)$–$f_4(y)$, were shown in the previous papers.[3b,5a]

D_D and R (C'_CK/k_D) were calculated from the slope and the intercept of the linear relationship in Figure 10, and F ($=D_C/D_D$) was obtained from this R and the above determined FR (Table III). The diffusivity for the Langmuir mode is 1–3% of the diffusivity for the Henry's mode.

Effect of Oxygen-Binding Capability of the Fixed Carrier on the Oxygen Permeability. The permeability coefficients (Figure 11) and the time lags for the POMPy–CoS membrane have been also measured and were analyzed according to the dual-mode transport theory, as well as for the POMIm–CoS membrane (Table III). The oxygen-binding affinity of the POMPy–CoS complex is smaller than that of the POMIm–CoS complex (Figure 5 and Table I) probably due to lower basicity of the pyridine ligand.[9] Therefore, it is assumed that the Langmuir population of the second term in eq 2 acts more effectively for POMIm–CoS than for POMPy–CoS. However, even at 25 °C P_{O_2} depends on $p_2(O_2)$ in the POMPy–CoS membrane (Figure 11), while P_{O_2} does not in the POMIm–CoS membrane (Figure 7). The F value at 25 °C was calculated to be ~0 for POMIm–CoS, although it was found to be 0.01 for POMPy–CoS (Table III). This is due

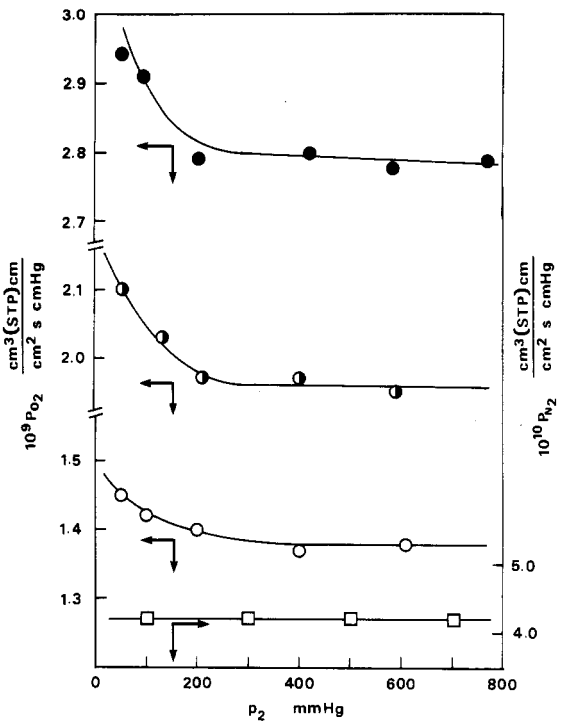

Figure 11. Effect of upstream gas pressure on permeation coefficient for the POMPy–CoS membrane: oxygen at 25 (○), 35 (◑), 45 °C (●); nitrogen at 25 °C (□); [CoS] = 0.6 wt %.

to the fact that the k_{off} value for POMPy–CoS is larger than that for POMIm–CoS at 25 °C, as has been shown in Table II.

On the other hand, the $p_2(O_2)$ dependency of P_{O_2} of POMIm–CoS is larger than that of POMPy–CoS at 45 °C because of the higher oxygen-binding affinity and the relatively large oxygen desorption rate constant at the same temperature as shown in Table II.

The saturated amounts of oxygen reversibly bound to the fixed carrier, C'_C values, are also given in Table III. The calculated C'_C values are independent of temperature. In the case of glassy polymers the Langmuir sorption capacity (C'_H) is based on the frozen free volume in the polymers. The frozen free volume or microvoid arises from the nonequilibrium nature of the polymers in a glassy state, and a quantitative uncertainty remains in the C'_H value, which decreases with time, temperature, pressure, and so on. On the other hand, in the membrane of the polymer-coordinated CoS the C'_C value in eq 2, which is corresponding to C'_H for glassy polymers, can be calculated to be a constant.

The C'_C value in POMPy–CoS is about twice that in POMIm–CoS, although the feed CoS concentration in the membrane is the same for both. This is probably because the POMIm ligand with greater basicity partially forms the six-coordinate CoS complex without oxygen-binding ability (This has been suggested above in the section on the coordination structure.)

Effect of the Fixed Carrier Concentration on the Oxygen Permeability and the Time Lag. Figure 12 shows the effect of the fixed carrier concentration in the POMPy–CoS membrane on the oxygen permeability coefficient. P_{O_2} decreases with the fixed carrier concentration. T_g of the POMPy–CoS membrane increased from −1 to 11 °C with the fixed carrier concentration. The decrease in P_{O_2} with CoS concentration is explained by the hardening effect of the additive, here the fixed carrier, on the polymer domain. However, the $p_2(O_2)$ dependency of P_{O_2} increases with fixed carrier concentration. This cor-

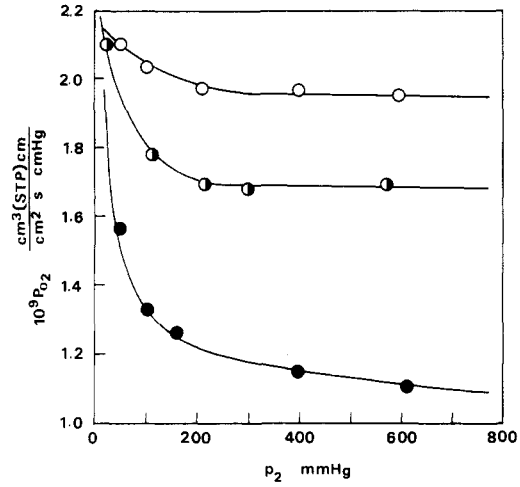

Figure 12. Effect of fixed carrier (CoS) concentration of $p_2(O_2)$ dependency of permeation coefficient for the POMPy–CoS membrane at 35 °C: [CoS] = 0.6 (○), 2.5 (◑), 8.0 wt % (●).

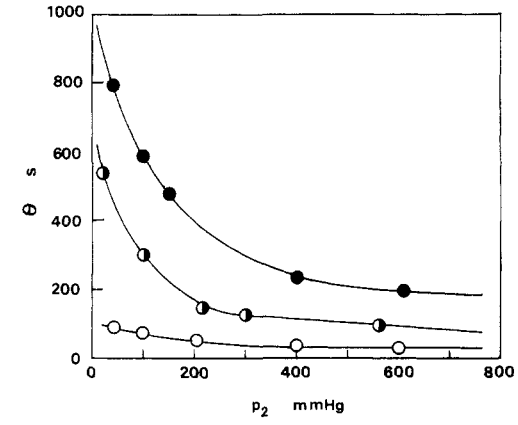

Figure 13. Effect of fixed carrier (CoS) concentration on $p_2(O_2)$ dependency of time lag for the POMPy–CoS membrane at 35 °C: [CoS] = 0.6 (○), 2.5 (◑), 8.0 wt % (●).

responds to eq 2 from which it is easily understood that the increase in the saturated amount of the oxygen reversibly bound to the fixed carrier, C'_C, contributes effectively to the facilitated oxygen transport by Langmuir's population.

Figure 13 shows that the time lag is increased with fixed carrier concentration because the fixed carrier interacts with the penetrant and retards its diffusivity in the membrane.

The oxygen permeability coefficients and time lags have been analyzed according to the dual mode transport theory as described above, and the parameters calculated are given in Table IV. The diffusion coefficient through the polymer domain, D_D, decreases with CoS concentration because of the hardening effect of the polymer domain by the additive as mentioned above. But the F ($=D_C/D_D$) value increases with CoS concentration. The diffusion coefficient via the fixed carrier, D_C, is not much influenced by the CoS concentration, because the ad- and desorption rate constants of oxygen to and from the fixed carrier are not directly affected by the hardening of polymer domain. Although the saturated amount of oxygen reversibly bound

Table IV
Dual-Mode Transport Parameters for the POMPy–CoS Membrane[a]

C, wt %	D_D, cm^2/s	D_C, cm^2/s	$F(D_C/D_D)$	k_D, $cm^3(STP)/cm^3$ cmHg	C'_C, $cm^3(STP)/cm^3$
0.6	2.6×10^{-6}	3.6×10^{-8}	0.01	7.4×10^{-4}	0.2
2.5	4.3×10^{-7}	1.1×10^{-8}	0.03	3.8×10^{-3}	2.0
8.0	2.2×10^{-7}	1.0×10^{-8}	0.05	4.8×10^{-3}	2.7

[a] At 35 °C, $K = 0.26\ cm^{-1}$

Table V
Oxygen Permeability Coefficient (at 35 °C) and Permeability Ratio (P_{O_2}/P_{N_2})

CoS in POMPy, wt %	permeability coeff[a]	P_{O_2}/P_{N_2}
0	1.95	2.3
0.6	2.56	3.5
2.5	2.65	4.8
8.0	3.12	6.5
12.0	1.47	15

[a] Upstream pressure, 10.0 mmHg. The permeability coefficient is expressed in units of (cm^3(STP) cm/cm^2 s cmHg) $\times 10^9$.

to the fixed carrier, C'_C, does not completely correspond to the fixed carrier concentration, C'_C certainly increases with fixed carrier concentration.

Effect of the fixed carrier concentration in the membrane on the permselectivity is shown in Table V. The permeability ratio (P_{O_2}/P_{N_2}) increases with CoS concentration and is above 10 for the membrane containing 12 wt % CoS at the upstream pressure 10.0 mmHg, which supports the theoretical prediction that the increase in C'_C of eq 2 contributes effectively to the Langmuir term and the facilitated transport. This result indicates a possibility of high permselectivity in a membrane containing a fixed carrier.

Acknowledgment. This work was partially supported by a Grant-in-Aid for Scientific Research on Priority Area "macromolecular complexes" from the Ministry of Education, Science and Culture, Japan.

Registry No. O_2, 7782-44-7.

References and Notes

(1) (a) Pusch, W.; Walch, A. *Angew. Chem., Int. Ed. Engl.* **1982**, *10*, 81. (b) Schell, W. J. *J. Membr. Sci.* **1985**, *22*, 217.
(2) (a) Comyn, J., *Ed. Polymer Permeability*; Elsevier: New York, 1985. (b) Kesting, R. E. *Synthetic Polymeric Membrane*, 2nd ed.; McGraw-Hill: New York, 1985.
(3) (a) Nishide, H.; Ohyanagi, M.; Okada, O.; Tsuchida, E. *Macromolecules* **1986**, *19*, 494. (b) Nishide, H.; Ohyanagi, M.; Okada, O.; Tsuchida, E. *Macromolecules* **1987**, *20*, 417.
(4) (a) Nishide, N.; Kuwahara, M.; Ohyanagi, M.; Funada, Y.; Kawakami, H.; Tsuchida, E. *Chem. Lett.* **1986**, *43*. (b) Nishide, H.; Ohyanagi, M.; Kawakami, H.; Tsuchida, E. *Bull. Chem. Soc. Jpn.* **1986**, *59*, 3213.
(5) (a) Paul, D. R.; Koros, W. J. *J. Polym. Sci. Polym. Phys. Ed.* **1976**, *14*, 675. (b) Paul, D. R. *Ber. Bunsenges. Phys. Chem.* **1979**, *83*, 294.
(6) Bailes, R. H.; Calvin, M. *J. Am. Chem. Soc.* **1947**, *69*, 1886.
(7) Chikira, M.; Migita, K.; Kawakita, T.; Iwaizumi, M.; Isobe, T. *J. Chem. Soc., Chem. Commum.* **1976**, 316.
(8) Tsuchida, E. *J. Macromol. Sci. Chem.* **1979**, *A13*, 545.
(9) Jones, R. D.; Summerville, D. A.; Basolo, F. *Chem. Rev.* **1979**, *79*, 319.